Journal of Hazardous Materials 168 (2009) 1217–1222

Contents lists available at ScienceDirect

Journal of Hazardous Materials

journal homepage: www.elsevier.com/locate/jhazmat

Adsorption and desorption hysteresis of 4-nitrophenol on a hyper-cross-linked polymer resin NDA-701

Changhong Hong[a], Weiming Zhang[a,b,c,*], Bingcai Pan[a], Lu Lv[a], Yongzhong Han[a], Quanxing Zhang[a,b,c]

[a] State Key Laboratory of Pollution Control and Resources Reuse, School of the Environment, Nanjing University, Nanjing 210093, PR China
[b] Jiangsu Engineering Research Center for Organic Pollution Control and Resources Reuse, Nanjing 210046, PR China
[c] State Environmental Protection Engineering Center for Organic Chemical Industrial Waste Water Disposal and Resources Reuse, Nanjing 210046, PR China

ARTICLE INFO

Article history:
Received 2 October 2008
Received in revised form 11 February 2009
Accepted 15 February 2009
Available online 13 March 2009

Keywords:
Desorption
Hysteresis
Hyper-cross-linked resin
4-Nitrophenol

ABSTRACT

Removal and recovery of aromatic pollutants from water by solid adsorbents have been of considerable concern recently. Relatively limited information is available on desorption kinetics and isotherms aspects. In the present study, batch desorption experiments of loaded 4-nitrophenol on a hyper-cross-linked polymer resin NDA-701, a polymeric adsorbent Amberlite XAD-4 and a granular activated carbon GAC-1 were carried out to study the effects of reaction temperature and pore-size distribution of adsorbents. 4-Nitrophenol desorbed rapidly in the early stages, followed by a much slower release, which was described well by a first-order two-component four-parameter model. The adsorption and desorption equilibrium isotherms were well described by Freundlich equation and the apparent adsorption–desorption hysteresis (hysteresis index) for 4-nitrophenol followed an order as: NDA-701 ≈ XAD-4 ≪ GAC-1. Analysis of adsorption–desorption process suggested that higher reaction temperature and larger proportion of macropore of adsorbents favoured desorption kinetic and reduced adsorption–desorption hysteresis. All the results indicated that NDA-701, with a specific bimodal property in macro- and micropore region, had excellent potential as an adsorption material for achieving high removal and recovery of 4-nitrophenol from the contaminated water. These results will also advance the understanding of the adsorption and desorption behavior of hyper-cross-linked polymer resin in the wastewater treatment systems.

1. Introduction

Water pollution by synthetic aromatic compounds has increasingly leaded an important environmental issue associated negatively with the health and economy, particularly in developing countries such as China [1]. Methods to remove aromatic pollutants from the contaminated waters are classified as recovery (e.g., adsorption, solvent extraction, and membrane separation) or destruction (e.g., chemical oxidation, electrolysis, and biodegradation) techniques [2–7]. Adsorption with easy and inexpensive regeneration is a desirable means to control the emissions of aromatic pollutants from industrial wastewaters as it allows for capture, recovery and reuse of those compounds [8]. However, when recovery and reuse of some aromatic compounds is not technically or economically feasible, transforming those into more environmentally friendly compounds can be more appropriate.

Activated carbons and synthetic polymer resins have been used for liquid purification and wastewater treatment [9–11]. Much attention has focused on the factors controlling the magnitude of adsorption in single-step uptake experiments [12], while little attention has been paid on the desorption steps [13–16]. Generally, the feasibility of an adsorptive removal process greatly depends on the cost of regeneration of spent adsorbents. It is well known that regeneration of activated carbons loaded with aromatic compounds is difficult, due to the strong adsorption–desorption hysteresis with the "pore deformation" [17]. Although the adsorption capacity of activated carbons is generally larger than that of most synthetic adsorbents, they are disadvantageous for certain applications because of their expensive regeneration. Hence, desorption characteristics are very important and necessary for selecting a suitable adsorbent and accessing an adsorption technology.

In the past few decades, hyper-cross-linked polymer resins invented by Davankov in the 1970s [18] have attracted increasing attention as an alterative to activated carbon in industrial effluent treatment mainly due to their superior mechanical rigidity, high surface area, adjustable matrix, and pore structure [19]. Similar with study on activated carbon, many researchers have investigated the factors controlling the adsorption prop-

* Corresponding author at: State Key Laboratory of Pollution Control and Resources Reuse, School of the Environment, Nanjing University, Nanjing 210093, PR China. Tel.: +86 25 83685736; fax: +86 25 83707304.
E-mail address: wmzhang@nju.edu.cn (W. Zhang).

0304-3894/$ – see front matter © 2009 Elsevier B.V. All rights reserved.
doi:10.1016/j.jhazmat.2009.02.161

erties of hyper-cross-linked polymer resins. Whereas, little is known about their adsorption–desorption kinetics and isotherms in the industrial wastewater treatment and liquid purification [20–23].

Recently, some desorption methods have been widely studied, including thermal (heating) [24,25] and chemical regeneration (organic solvents or inorganic chemicals) [26,27]. A number of desorption systems have been observed to exhibit a biphasic behavior with two distinct time scales: a rapid release in the order of minutes followed by a slow time scale in the order of hours to days or even weeks [28,29]. In most cases, non-linearity was observed in the desorption isotherms and was described by the empirical Freundlich model [30]. However, little has been done to determine the impacts of pore-size distribution of adsorbents and reaction temperature on desorption kinetics and isotherms for hyper-cross-linked polymer resins. An understanding of the impacts will benefit the development of an efficient removal process, as well as the prospect for a successful recovery process.

In the present study, batch desorption kinetics and isotherms of 4-nitrophenol (denoted 4-NP hereafter) on a hyper-cross-linked polymeric adsorbent (NDA-701) in aqueous solution were performed compared to two widely used adsorbents in field application, a polymeric adsorbent (Amberlite XAD-4) and commercial activated carbon (GAC-1). As an important nitroaromatic compound but well-known priority pollutant, 4-NP was selected for this study and its adsorption equilibrium and kinetics have been discussed in previous papers [31]. The objectives of this research were to gain an improved understanding of the desorption process, to evaluate the impacts of reaction temperature and pore-size distribution on the 4-NP removal and recovery kinetics and capacities, and to quantify the adsorption–desorption hysteresis, and to access NDA-701 as a potential adsorption material for removal and recovery of 4-nitrophenol from the contaminated water.

2. Materials and methods

2.1. Materials

4-Nitrophenol (4-NP) and other reagents were purchased from Shanghai Reagent Station (Shanghai, China) in A.R. grade and used without further purification. A hyper-cross-linked adsorbent NDA-701 was prepared according to our previous study [31]. The polymeric adsorbent Amberlite XAD-4 was kindly provided by Rohm and Haas (USA), and a coconut-shell granular activated carbon GAC-1 was purchased from Jinbei Fine Chemical Co. (Tianjin, China).

Detailed physiochemical properties of the adsorbents used in this study are presented in Table 1 [31]. Table 1 and the pore-size distribution plots of three adsorbents (not shown) [31] indicated that NDA-701 provides a specific bimodal property in macro- and micropore region, GAC-1 dominates in the micropore region, while the mesopore region plays the main role for XAD-4.

Prior to use, all the adsorbents were packed in column and first rinsed with 10 bed volumes (BV) of 1.0N HCl followed by D.I. washing till neutral pH. Then the column was subjected to acidic flushing by introducing 10 BV of 1.0N NaOH and again D.I. flushing to neutral pH. Finally, the adsorbents except for GAC-1 were extracted with ethanol for 4 h in a Soxlet apparatus, and all the adsorbents were vacuum desiccated at 325 K for 8 h before use.

2.2. Adsorption and desorption equilibrium experiments

Equilibrium adsorption experiments were carried out at 303 K in 100-mL glass flasks. 0.050 g of adsorbent particles was introduced to a 50 mL solution containing known 4-NP concentrations (1, 2, 3, 4, 5, and 6 mmol L^{-1}, respectively). The flasks were then transferred to a G 25 model incubator shaker with thermostat (New Brunswick Scientific Co. Inc.) and shaken under 200 rpm until the adsorption process reached equilibrium, as indicated by our previous kinetic study [31]. The supernatants were analyzed to determine the 4-NP distribution between the solid and solution phases.

Immediately after adsorption, desorption equilibrium experiments were carried out on the systems with different 4-NP loadings by replacing the removed 25 mL equilibrium aliquots with the same volume of 4-NP-free distilled water at 303 K. This process resulted in dilution of the 4-NP concentration in the solutions and thus perturbation of the pre-established equilibria. The systems were subsequently shaken for another 24 h, reequilibrated, and the supernatants were analyzed to determine the new 4-NP distribution between the solid and solution phases. Preliminary 4-NP release kinetic tests showed that pseudo-equilibrium states were established within 24 h in the systems.

The desorption cycles were repeated five times and then desorption isotherms were prepared by plotting the amounts of 4-NP remained in the solid phase after each desorption cycle vs. the corresponding equilibrium 4-NP concentrations in solution.

Adsorbed and desorbed concentrations were calculated by the difference in mass added (or mass remaining, in the case of desorption) and mass in solution, applying a correction for "bottle losses". The solution remained on the surface of adsorbents and in their pores after the filtration. In this work, the amount of solu-

Table 1
Main properties of adsorbents used in this study[a] [31].

Adsorbent	GAC-1	NDA-701	XAD-4
Matrix	Coconut-shell-based	St-DVB	St-DVB
Average pore diameter (nm)	2.23	2.24	5.61
BET surface area ($m^2\ g^{-1}$)			
Total	790	824	886
Macropore area	114	306	196
Mesopore area	105	88	651
Micropore area	571	430	39
Pore volume ($cm^3\ g^{-1}$)	0.52	0.58	1.22
Micropore volume ($cm^3\ g^{-1}$)	0.22	0.22	0.0043
Density (wet, g mL^{-1})	1.05	1.08	1.04
Particle size (mm)	0.3–0.6	0.5–1.0	0.5–1.0
Swelling ratio in benzene (%)	NA	<5	>15
Osmotic-attrited perfect ball ratio (%)	NA	>99.5	>92

[a] The parameters (volume and area) of porous structure were measured by using nitrogen adsorption on ASAP-2010C Micromeritics Instrument (USA), and then calculated by BJH and HK models with Autosorb 1.0 software of Quantachrome Corporation.

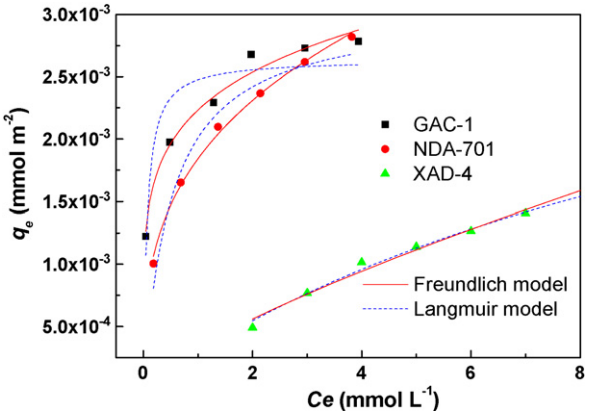

Fig. 1. Adsorption isotherms of 4-NP on GAC-1, NDA-701, and XAD-4 at 303 K.

tion remained was much smaller than the amount of distilled water used in the desorption experiments. We did not control the solution pH in the adsorption and desorption experiments. The detailed pH variety and its slight effect on 4-NP adsorption/desorption on the three adsorbents are listed and discussed in the supporting information.

2.3. Desorption kinetics experiments

To start the experiment, 0.400 g of adsorbent particles was introduced to a 400 mL solution containing 6 mmol L^{-1} 4-NP in a 1000-mL glass bottle. The flask was then transferred to a G 25 model incubator shaker with thermostat (New Brunswick Scientific Co. Inc.) and shaken under 200 rpm for 24 h at 303 K.

After adsorption, the spent adsorbent particles were filtered from the solution and 400 mL of 4-NP-free distilled water was used for desorption at 303, 318, and 333 K. A 0.5 mL aliquot of solution was sampled from the flask at various time intervals to determine desorption kinetics.

2.4. Analysis

All the concentrations of 4-NP in aqueous solution were determined spectrophotometrically using a Helious Betra UV–vis spectrophotometer (U.K.) at wavelength of 400 nm. Before analysis, pH of all the samples was adjusted to 10 ± 0.5 to minimize the disturbing effect of solution pH [31].

3. Desorption isotherms and kinetics models

3.1. Desorption isotherms model

Adsorption and desorption isotherms were fitted to the Freundlich equation using the non-linear least square analysis. The Freundlich equation can be presented in adsorption and desorption processes as [30]:

$$q_e = K_F C_e^{1/n_F} \quad (1)$$

$$q_e = K_{Fd} C_e^{1/n_{Fd}} \quad (2)$$

where q_e (mmol g^{-1}) is the equilibrium concentration in solid phase, C_e (mmol L^{-1}) represents the equilibrium concentration in aqueous phase, K_F and n_F are Freundlich adsorption constants, and K_{Fd} and n_{Fd} are Freundlich desorption constants.

Finally, each couple of adsorption and desorption isotherms was compared to evaluate their singularity and the following index was calculated when hysteresis observed in the adsorption and desorption isotherms [33]:

$$H = \frac{n_{Fd}}{n_F} \quad (3)$$

3.2. Desorption kinetics model

A phenomenological first-order two-component four-parameter model comprising both fast and slow desorption steps was used to describe the desorption rate of 4-NP from adsorbents [32]:

$$\frac{q_{dt}}{q_{de}} = F_1 \exp(1 - k_1 t) + F_2 \exp(1 - k_2 t) \quad (4)$$

where F_1 and F_2 are the rapidly and slowly desorbing fractions, respectively. The rate constants of rapid and slow desorption are designated as k_1 and k_2 (min^{-1}). This model is widely applied in various desorption systems due to its simplicity and was found to be adequately describing desorption of various samples with different characteristics. The parameters from the model are useful for distinguishing between rapidly and slowly desorbing fractions. Furthermore, results from the models gave the biphasic nature of desorption data in this study. However, it should be noted that this model does not necessarily have a mechanistic meaning, i.e., it is uncertain whether the rapid and slow desorption corresponded to a physicochemical process [29].

4. Results and discussion

4.1. Adsorption isotherms

Adsorption isotherms of 4-NP onto three adsorbents (in Fig. 1) are represented by the Freundlich model and Langmuir model. Results in Table 2 showed that the Freundlich model represents all the 4-NP adsorption isotherms more reasonably than the Langmuir one. K_F and n_F values shown in Table 2 are observed in sequence as GAC-1 > NDA-701 > XAD-4. The highest adsorption capacity and affinity of GAC-1 than NDA-701 and XAD-4 was assumed to result from the largest micropore surface, where 4-NP can be intensively adsorbed by micropore filling mechanism. On the other side, adsorption of 4-NP in molecular state from aqueous systems to polystyrene adsorbents NDA-701 and XAD-4 generally is mainly driven by hydrophobic interaction as well as π–π interaction between adsorbent and adsorbate. However, the significant higher adsorption capacity and affinity of NDA-701 than XAD-4 also was probably due to the larger micropore structure with the extra micropore filling interaction. This is consistent with our previous study [31].

4.2. Desorption isotherms

Adsorption and desorption isotherms were compared to assess the degree of reversibility of adsorption reaction. A comparison of these isotherms does provide an assessment of structure characteristics of adsorbent on the desorption behavior of 4-NP. Fig. 2 shows adsorption equilibria and desorption data of 4-NP on GAC-1, NDA-701, and XAD-4. The ordinate is the amount adsorbed, and the abscissa is the relative concentration. Filled symbols and open symbols denote adsorption and desorption data. We calculated the hysteresis index (H), defined as the n_{Fd}/n_F ratio [33], to quantify the degree of apparent adsorption–desorption hysteresis. The H values for all of the adsorbents with different 4-NP loadings are listed in Table 3.

The highly non-linear adsorption isotherm and relatively flat desorption isotherm in Fig. 2 provide visual evidence of apparent adsorption–desorption hysteresis ($H > 2$) on GAC-1. The hysteresis

Table 2
Isotherm parameters of 4-NP adsorption on GAC-1, NDA-701, and XAD-4 at 303 K.

Adsorbent	Freundlich				Langmuir			
	K_F	n_F	R^2	x^2	K_L (L mmol^{-1})	q_m (mmol g^{-1})	R^2	x^2
GAC-1	1.764 ± 0.0317	5.420 ± 0.4556	0.981	0.0053	14.968 ± 6.2925	2.086 ± 0.1093	0.855	0.0411
NDA-701	1.518 ± 0.0186	3.066 ± 0.1130	0.996	0.0014	1.951 ± 0.4416	2.504 ± 0.1396	0.961	0.0149
XAD-4	0.592 ± 0.0158	2.124 ± 0.0968	0.994	0.0006	0.528 ± 0.0701	1.674 ± 0.0879	0.989	0.0012

Table 3
Freundlich desorption constants (K_{Fd} and n_{Fd}) for desorption of loaded 4-NP on adsorbents by distilled water, and hysteresis indices (H).

Adsorbent	Sample	K_{Fd}	n_{Fd}	H[a]	R^2	x^2
GAC-1	D1	1.067 ± 0.0223	32.737 ± 5.8991	6.040	0.885	0.00002
	D2	1.663 ± 0.0176	12.875 ± 0.9934	2.376	0.977	0.00017
	D3	1.786 ± 0.0083	11.522 ± 0.5409	2.126	0.991	0.00015
	D4	2.018 ± 0.0116	11.677 ± 0.8350	2.154	0.980	0.00053
	D5	1.961 ± 0.0047	10.927 ± 0.3233	2.016	0.997	0.00012
	D6	1.978 ± 0.0116	11.612 ± 0.8662	2.143	0.978	0.00079
NDA-701	D1	1.643 ± 0.0213	2.466 ± 0.0382	0.804	0.999	0.00001
	D2	1.562 ± 0.0112	2.862 ± 0.0557	0.933	0.998	0.00007
	D3	1.577 ± 0.0102	3.091 ± 0.0915	1.008	0.997	0.00032
	D4	1.563 ± 0.0095	3.276 ± 0.1027	1.068	0.996	0.00050
	D5	1.579 ± 0.0105	3.399 ± 0.1038	1.109	0.996	0.00061
	D6	1.622 ± 0.0139	3.592 ± 0.1276	1.171	0.995	0.00098
XAD-4	D1	0.597 ± 0.0079	1.710 ± 0.0320	0.805	0.999	0.00002
	D2	0.580 ± 0.0040	1.869 ± 0.0350	0.880	0.999	0.00005
	D3	0.641 ± 0.0066	2.217 ± 0.0721	1.044	0.996	0.00023
	D4	0.625 ± 0.0084	2.281 ± 0.0825	1.074	0.995	0.00036
	D5	0.631 ± 0.0108	2.359 ± 0.0954	1.111	0.994	0.00056
	D6	0.652 ± 0.0097	2.408 ± 0.0758	1.134	0.997	0.00042

[a] $H = n_{Fd}/n_F$.

suggests the adsorption irreversibility in aqueous solution for granular activated carbon in consent with many other studies [34,35]. On the other hand, isotherm results show that no hysteresis is observed for the synthetic polymeric adsorbent XAD-4, and the adsorption is reversible in aqueous solution (H is about 1). This is because XAD-4 has a negligible proportion of micropores, whereas in GAC-1 essentially all pores existed as micropores of <2 nm width. These micropores probably entrap the loaded 4-NP molecule and cause a slow and prolonged adsorption–desorption process, which may have led to the apparent adsorption–desorption hysteresis due to non-equilibrium processes. Yu et al. [36] assessed the well relationship between the microporosity and apparent desorption hysteresis exists in diuron adsorption–desorption on soils. Braida et al. [17] noted swelling of an adsorbent during benzene adsorption and suggested pore deformation during desorption causing desorption hysteresis.

Hyper-cross-linked polymeric resin NDA-701, with much micropore and macropore, interestingly also presents no adsorption–desorption hysteresis for 4-NP in the aqueous solution. It is probably due to the specific bimodal property in macro- and micropore region of NDA-701. The macropore of NDA-701 would function as a wide pathway for 4-NP molecule diffusing in or out the micropore region of the microgels, and therefore improve the adsorption–desorption kinetics as well as reduce adsorption–desorption hysteresis. The results showed that besides the high adsorption capacity, NDA-701 had good desorption performance essentially without adsorption–desorption hysteresis, which indicated NDA-701 as a potential adsorption material for removal and recovery of 4-NP from the contaminated water.

On the other hand, the test tree adsorbents (GAC-1, NDA-701, and XAD-4) have different surface chemistry [31], which also obviously result in the different affinity to 4-NP. The role of surface chemistry of adsorbents on adsorption–desorption hysteresis and the following kinetics should be systemically investigated in our near future research.

4.3. Desorption kinetics

Desorption kinetic curves of loaded 4-NP on GAC-1, NDA-701, and XAD-4 by 4-NP-free distilled water are presented in Fig. 3. The 4-NP release process was rapid in the first ≈50 min for GAC-1, ≈30 min for NDA-701, ≈15 min for XAD-4, respectively, and then continued with a slower rate. The rate of approach to equilibrium follows an order as: GAC-1 < NDA-701 < XAD-4. However, about 800 min of contact time is still enough for all the three adsorbents to ensure 4-NP desorption equilibrium. Additionally, an increase in reaction temperature from 303 to 333 K observably augmented and speeded the 4-NP release process. The different desorption rates including rapid and slow steps show that the pore-size distribution of adsorbents and reaction temperature may play a dominant role on 4-NP desorption on the spent adsorbents by water.

Desorption kinetic data for all the adsorbents were also successfully described by a phenomenological first-order two-component four-parameter model. Desorption kinetic parameters determined from the model are listed in Table 4. As shown in Table 4, both rapid and slow desorption rates and fractions were strong functions of pore-size distribution and reaction temperature. Firstly, the 4-NP release process was distinctly divided into two steps, because the k_2 (slow) value of each system was up to two or three

Table 4
Desorption kinetic parameters of 6 mmol L^{-1} 4-NP from GAC-1, NDA-701, and XAD-4.

Adsorbent	T (K)	F_1	k_1 (min^{-1})	F_2	k_2 (min^{-1})	R^2	x^2
GAC-1	303	0.159 ± 0.0032	0.0481 ± 0.0025	0.815 ± 0.0026	0.00005 ± 0.00001	0.995	0.00002
	318	0.171 ± 0.0049	0.0615 ± 0.0040	0.772 ± 0.0031	0.00005 ± 0.00001	0.992	0.00003
	333	0.174 ± 0.0063	0.0981 ± 0.0073	0.746 ± 0.0032	0.00006 ± 0.00002	0.988	0.00003
NDA-701	303	0.250 ± 0.0103	0.0481 ± 0.0044	0.741 ± 0.0106	0.00043 ± 0.00008	0.993	0.00009
	318	0.326 ± 0.0044	0.0592 ± 0.0018	0.652 ± 0.0046	0.00049 ± 0.00006	0.999	0.00001
	333	0.415 ± 0.0049	0.0872 ± 0.0023	0.549 ± 0.0051	0.00060 ± 0.00012	0.999	0.00002
XAD-4	303	0.520 ± 0.0071	0.0885 ± 0.0029	0.391 ± 0.0069	0.00056 ± 0.00017	0.999	0.00005
	318	0.545 ± 0.0122	0.1766 ± 0.0098	0.314 ± 0.0092	0.00142 ± 0.00036	0.996	0.00014
	333	0.585 ± 0.0078	0.2256 ± 0.0068	0.242 ± 0.0054	0.00159 ± 0.00046	0.999	0.00005

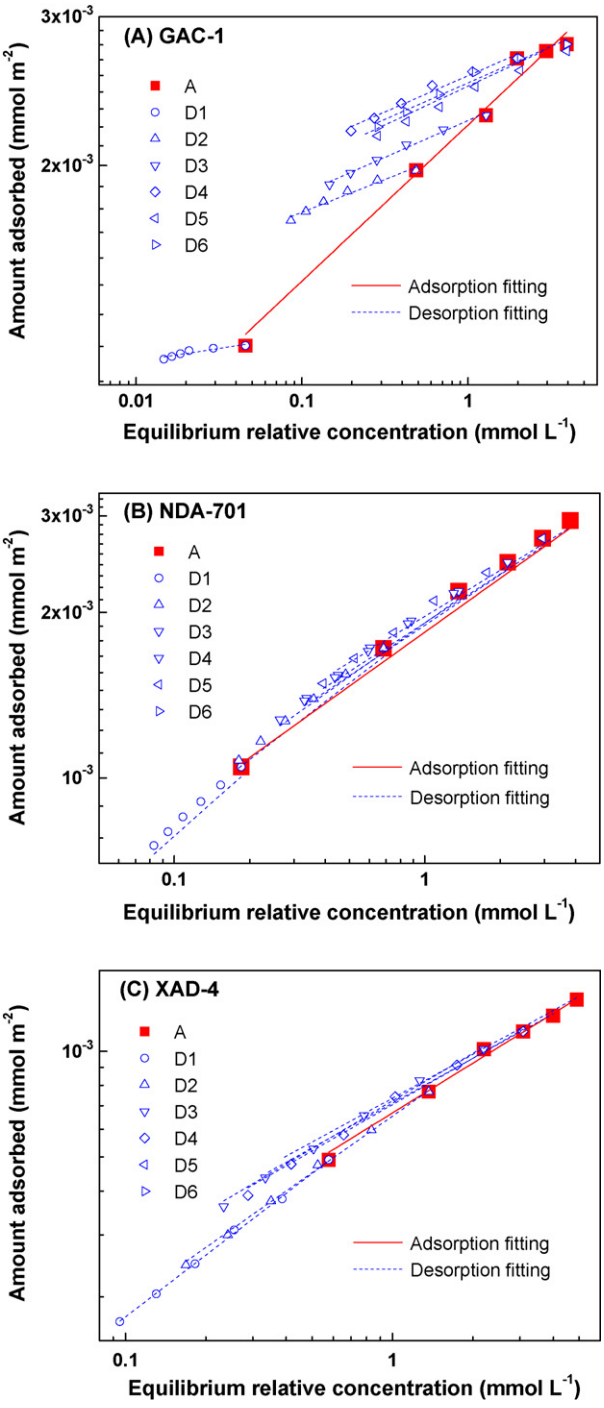

Fig. 2. Adsorption–desorption isotherms of 4-NP on GAC-1, NDA-701, and XAD-4 in distilled water. (Filled symbols correspond to adsorption, and unfilled symbols correspond to desorption.)

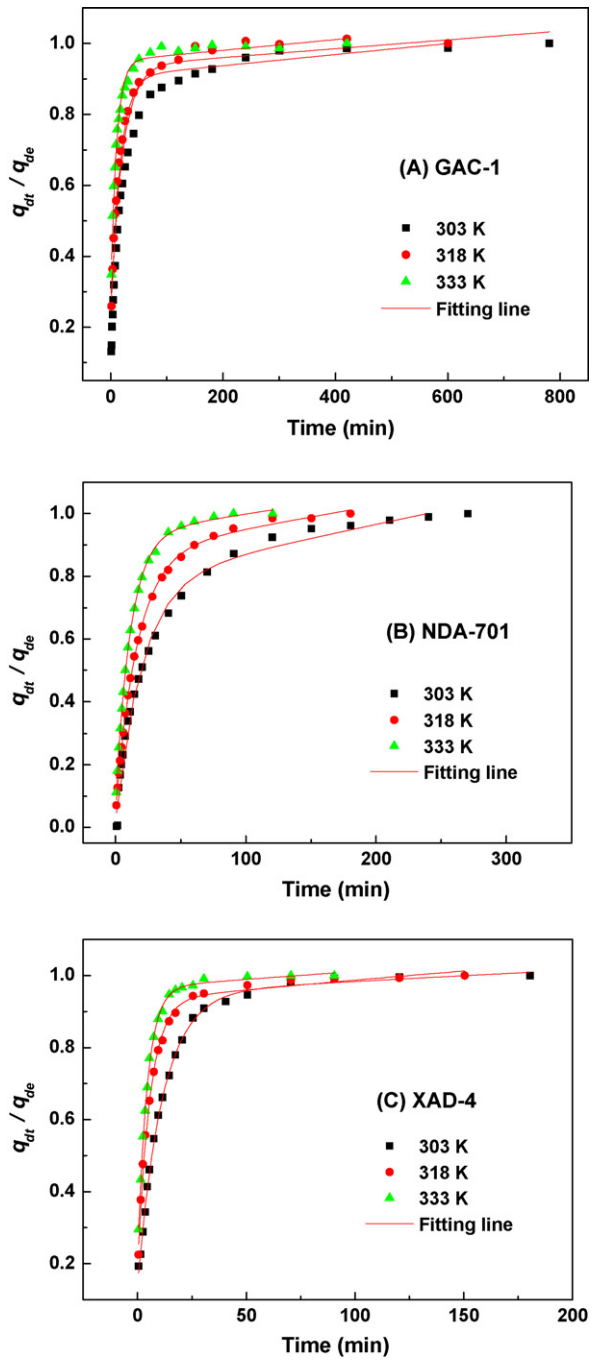

Fig. 3. Effect of contact time on 4-NP desorption on GAC-1, NDA-701, and XAD-4 by distilled water.

orders of magnitude lower than the corresponding k_1 (rapid) value. For all the test systems, the F_1 value of the rapid desorption fraction follows an order as GAC-1 > NDA-701 > XAD-4; while, their corresponding F_2 value of the slow fraction are in sequence as GAC-1 < NDA-701 < XAD-4. These results indicate that (1) the extent of rapid desorption was more prominent on XAD-4 due to its dominated mesopore structure; (2) the desorption processes on GAC-1 are limited mainly by the slow desorption attributed to its abundant microspore structure; (3) the adsorption process on NDA-701 is controlled by both rapid and slow desorption according to its specific bimodal property in macro- and micropore region. Secondly, when the reaction temperature increases, both k_1 and k_2 values increased, and the F_1 value of the rapid desorption fraction also enlarged, whereas the corresponding F_2 value of the slow desorption fraction reduced contrarily. Results show that the high reaction temperature helps to desorption rate and magnitude of the loaded 4-NP molecule especially in the macrospore region of adsorbents.

5. Conclusions

Due to its specific bimodal property in macro- and micropore region, NDA-701 presented high adsorption capacity and good desorption performance essentially without adsorption–desorption hysteresis. The desorption process of 4-NP from porous adsorbents

included rapid and slow stages. The experimental data for desorption kinetics corresponded well with a first-order two-component model. Higher reaction temperature and larger proportion of macropore of adsorbents favoured desorption kinetic and reduced adsorption–desorption hysteresis. The results from this study accessed NDA-701 as a potential adsorption material for removal and recovery of 4-NP from the contaminated water. The role of surface chemistry of adsorbents on adsorption–desorption kinetics and hysteresis should be systemically investigated in our near future research.

Acknowledgements

This research was financially funded by National Natural Science Funding of PR China (Grant No. 20744005), and Program for New Century Excellent Talents in University (NCET).

Appendix A. Supplementary data

Supplementary data associated with this article can be found, in the online version, at doi:10.1016/j.jhazmat.2009.02.161.

References

[1] G.W. Pan, T. Hanaoka, M. Yoshimura, S.J. Zhang, P. Wang, H. Tsukino, K. Inoue, H. Nakazawa, S. Tsugane, K. Takahashi, Decreased serum free testosterone in workers exposed to high levels of di-n-butyl phthalate (DBP) and di-2-ethylhexyl phthalate (DEHP): a cross-sectional study in China, Environ. Health Perspect. 114 (2006) 1643–1648.
[2] G.O. Yahaya, Separation of volatile organic compounds (BTEX) from aqueous solutions by a composite organophilic hollow fiber membrane-based pervaporation process, J. Membr. Sci. 319 (2008) 82–90.
[3] F.X. Pierre, I. Souchon, M. Marin, Recovery of sulfur aroma compounds using membrane-based solvent extraction, J. Membr. Sci. 187 (2001) 239–253.
[4] W.M. Zhang, C.H. Hong, B.C. Pan, L. Lv, Z.W. Xu, Q.J. Zhang, Removal enhancement of 1-naphthol and 1-naphthylamine in single and binary aqueous phase by acid-basic interactions with polymer adsorbents, J. Hazard. Mater. 158 (2008) 293–299.
[5] I. Sirés, E. Guivarch, N. Oturan, M.A. Oturan, Efficient removal of triphenylmethane dyes from aqueous medium by in situ electrogenerated Fenton's reagent at carbon-felt cathode, Chemosphere 72 (2008) 592–600.
[6] V.A. Alva, B.M. Peyton, Phenol and catechol biodegradation by the haloalkaliphile *Halomonas campisalis*: influence of pH and salinity, Environ. Sci. Technol. 37 (2003) 4397–4402.
[7] F. Mijangos, F. Varona, N. Villota, Changes in solution color during phenol oxidation by Fenton reagent, Environ. Sci. Technol. 40 (2006) 5538–5543.
[8] B.C. Pan, W.M. Zhang, B.J. Pan, H. Qiu, Q.R. Zhang, Q.X. Zhang, S.R. Zheng, Efficient removal of aromatic sulfonates from wastewater by a recyclable polymer: 2-naphthalene sulfonate as a representative pollutant, Environ. Sci. Technol. 42 (2008) 7411–7416.
[9] H. Tamon, M. Okazaki, Desorption characteristics of aromatic compounds in aqueous solution on solid adsorbents, J. Colloid Interf. Sci. 179 (1996) 181–187.
[10] M. Sanchez-Polo, J. Rivera-Utrilla, G. Prados-Joya, M.A. Ferro-Garcia, I. Bautista-Toledo, Removal of pharmaceutical compounds, nitroimidazoles, from waters by using the ozone/carbon system, Water Res. 42 (2008) 4163–4171.
[11] C. Valderrama, X. Gamisans, X. de las Heras, A. Farran, J.L. Cortina, Sorption kinetics of polycyclic aromatic hydrocarbons removal using granular activated carbon: intraparticle diffusion coefficients, J. Hazard. Mater. 157 (2008) 386–396.
[12] W.M. Zhang, Z.W. Xu, B.C. Pan, L. Lv, Q.J. Zhang, Q.R. Zhang, Q.X. Zhang, Assessment on the removal of dimethyl phthalate from aqueous phase using a hydrophilic hyper-cross-linked polymer resin NDA-702, J. Colloid Interf. Sci. 311 (2007) 382–390.
[13] J.A. Laszlo, Regeneration of azo-dye-saturated cellulosic anion exchange resin by *Burkholderia cepacia* anaerobic dye reduction, Environ. Sci. Technol. 34 (2000) 167–172.
[14] B. Gu, G.M. Brown, L. Maya, M.J. Lance, B.A. Moyer, Regeneration of perchlorate (ClO^{4-})-loaded anion exchange resins by a novel tetrachloroferrate ($FeCl^{4-}$) displacement technique, Environ. Sci. Technol. 35 (2001) 3363–3368.
[15] M. Bryjak, G. Poźniak, N. Kabay, Donnan dialysis of borate anions through anion exchange membranes: a new method for regeneration of boron selective resins, React. Funct. Polym. 67 (2007) 1635–1642.
[16] G.E. Üstün, S.K.A. Solmaz, A. Birgül, Regeneration of industrial district wastewater using a combination of Fenton process and ion exchange—a case study, Resour. Conserv. Recycl. 52 (2007) 425–440.
[17] W.J. Braida, J.J. Pignatello, Y.F. Lu, P.I. Ravikovitch, A.V. Neimark, B. Xing, Sorption hysteresis of benzene in charcoal particles, Environ. Sci. Technol. 37 (2003) 409–417.
[18] V.A. Davankov, M.P. Tsyurupa, Structure and properties of hypercrosslinked polystyrene—the first representative of a new class of polymer networks, React. Polym. 13 (1990) 27–42.
[19] M.P. Tsyurupa, V.A. Davankov, Hypercrosslinked polymers: basic principle of preparing the new class of polymeric materials, React. Funct. Polym. 53 (2002) 93–203.
[20] N. Fontanals, R.M. Marce, F. Borrull, Improved polymeric materials for more efficient extraction of polar compounds from aqueous samples, Curr. Anal. Chem. 2 (2006) 171–179.
[21] Z.W. Ming, C.J. Long, P.B. Cai, Z.Q. Xing, B. Zhang, Synergistic adsorption of phenol from aqueous solution onto polymeric adsorbents, J. Hazard. Mater. 128 (2006) 123–129.
[22] C. Valderrama, J.L. Cortina, A. Farran, X. Gamisans, F.X. de las Heras, Evaluation of hyper-cross-linked polymeric sorbents (Macronet MN200 and MN300) on dye (Acid red 14) removal process, React. Funct. Polym. 68 (2008) 679–691.
[23] C. Valderrama, J.L. Cortina, A. Farran, X. Gamisans, C. Lao, Kinetics of sorption of polyaromatic hydrocarbons onto granular activated carbon and Macronet hyper-cross-linked polymers (MN200), J. Colloid Interf. Sci. 317 (2007) 35–46.
[24] J.H. Kim, S.J. Lee, M.B. Kim, J.J. Lee, C.H. Lee, Sorption equilibrium and thermal regeneration of acetone and toluene vapors on an activated carbon, Ind. Eng. Chem. Res. 46 (2007) 4584–4594.
[25] M.Y. Cheng, S.C. Yang, C.T. Hsieh, Thermal regeneration of activated carbons exhausted with phenol compound, Sep. Sci. Technol. 42 (2007) 639–652.
[26] K. Rinkus, B.E. Reed, W. Lin, NaOH regeneration of Pb and phenol-laden activated carbon. 1. Batch study results, Sep. Sci. Technol. 32 (1997) 2367–2384.
[27] R. Qadeer, A.H. Rehan, A study of the adsorption of phenol by activated carbon from aqueous solutions, Turk. J. Chem. 26 (2002) 357–361.
[28] S.B. Hawthorne, D.G. Poppendieck, C.B. Grabanski, R.C. Loehr, PAH release during water desorption, supercritical carbon dioxide extraction, and field bioremediation, Environ. Sci. Technol. 35 (2001) 4577–4583.
[29] B.S. Chu, B.S. Baharin, Y.B.C. Man, S.Y. Quek, Separation of vitamin E from palm fatty acid distillate using silica. III. Batch desorption study, J. Food Eng. 64 (2004) 1–7.
[30] S.G. Paviostathis, G.N. Mathavan, Desorption kinetics of selected volatile organic compounds from field contaminated soils, Environ. Sci. Technol. 26 (1992) 532–538.
[31] B.C. Pan, W. Du, W.M. Zhang, X. Zhang, Q.R. Zhang, B.J. Pan, L. Lv, Q.X. Zhang, J.L. Chen, Improved adsorption of 4-nitrophenol onto a novel hyper-cross-linked polymer, Environ. Sci. Technol. 41 (2007) 5057–5062.
[32] M.D. Johnson, T.M. Keinath, W.J. Weber Jr., A distributed reactivity model for sorption by sails and sediments. 14. Characterization and modeling of phenanthrene desorption rates, Environ. Sci. Technol. 35 (2001) 1688–1695.
[33] M. Sanchez-Camazano, M.J. Sanchez-Martin, M.S. Rodriguez-Cruz, Sodium dodecyl sulphate-enhanced desorption of atrazine: effect of surfactant concentration and of organic matter content of soils, Chemosphere 41 (2000) 1301–1305.
[34] A.P. Terzyk, The effect of carbon surface chemical composition on the adsorption of acetanilide, J. Colloid Interf. Sci. 272 (2004) 59–75.
[35] S. Lagerge, J. Zajac, S. Partyka, A.J. Groszek, Comparative study on the adsorption of cyanide gold complexes onto different carbonaceous samples: measurement of the reversibility of the process and assessment of the active surface inferred by flow microcalorimetry, Langmuir 15 (1999) 4803–4811.
[36] X.Y. Yu, G.G. Ying, R.S. Kookana, Sorption and desorption behaviors of diuron in soils amended with charcoal, J. Agric. Food Chem. 54 (2006) 8545–8550.